Available online at www.sciencedirect.com
SCIENCE DIRECT®
PERGAMON
International Journal of Heat and Mass Transfer 46 (2003) 5099–5111
International Journal of HEAT and MASS TRANSFER
www.elsevier.com/locate/ijhmt

Effects of pore size distribution and fiber diameter on the coupled heat and liquid moisture transfer in porous textiles

Qingyong Zhu [a,b,*], Yi Li [b]

[a] School of Mathematics and Computational Science, Zhongshan University, Guangzhou 510275, China
[b] Institute of Textiles and Clothing, The Hong Kong Polytechnic University, Hung Hom, Kowloon, Hong Kong, China

Received 7 January 2003; received in revised form 18 June 2003

Abstract

The pore size distribution and the fiber diameter on the coupled heat and liquid moisture transfer in porous textiles are investigated to reveal the mechanisms of the coupling effects. This paper focuses on a theoretical investigation of the coupling mechanism of heat transfer and liquid moisture diffusion in porous textiles by using an improved mathematical model. In this model, the pore size distribution is assumed to be a cubic-polynomial distribution, which is close to the experimental measurements [Text. Res. J. 56 (1) (1986) 35]. The liquid diffusion behavior in porous textiles can be described as a diffusion equation. The improved diffusion coefficient can be expressed as: $D_l(\varepsilon_l) = \frac{5}{21}\frac{d_c}{\varepsilon}\frac{\sin^2\beta}{\eta}\frac{7\varepsilon-6\varepsilon_l}{5\varepsilon-4\varepsilon_l}\varepsilon_l\sigma\cos\phi$. For comparison, two types of pore distribution and the fiber diameter in the porous textiles are discussed. With specification of initial and boundary conditions, the distributions of the temperature, moisture concentration, and liquid water content in the porous textiles can be numerically computed. The comparison with the experimental measurements shows the superiority of this new model in resolving the coupled heat and liquid moisture transfer in porous textiles. The results illustrate that the heat transfer process is influenced by the pore size distribution and fiber diameter of the porous textiles.

1. Introduction

The pore size distribution and the fiber diameter present in a fibrous material often have significant impact on the moisture transport processes. Pore size distribution can influence the rate and magnitude of spontaneous uptake of liquids in porous textiles and control the flow pattern of a fluid moving through a porous material. The fiber diameter can influence the heat rate of sorption or desorption of water vapor by the fibers. Due to the much greater porosity range, the fibrous porous textiles, which have certain degree of moisture absorption capability (called hygroscopicity), have a much wider range in flow resistance than porous media made of granular particles. Given the fiber diameter and particle size, one can determine how much material is required for a porous media. Not so easily determined is permeability or flow resistance. The flow of the liquid moisture through the textiles is caused by fiber–liquid molecular attraction at the surface of the fiber materials, which is mainly determined by the surface tension and effective capillary pore distribution and pathways. Evaporation and/or condensation take place, depending on the temperature and moisture distributions. The heat transfer process is coupled with the moisture transfer processes with phase changes such as moisture sorption/desorption and evaporation/condensation.

Based on the filtration media properties, the Kozeny–Carman equation was developed to provide a description of fluid flow in the porous media. One form of this equation is

$$B = \frac{1}{K_0 S_0^2}\frac{\varepsilon^3}{(1-\varepsilon)^2}$$

* Corresponding author. Address: School of Mathematics and Computational Science, Zhongshan University, Guangzhou 510275, China. Tel.: +8620-8411-0192; fax: +8620-8403-6235.
E-mail address: qingyongzhu@yahoo.com (Q. Zhu).

0017-9310/$ - see front matter © 2003 Elsevier Ltd. All rights reserved.
doi:10.1016/S0017-9310(03)00370-3

Nomenclature

A_c	cross-sectional flow area (m^2)
B	permeability of the porous media (m^2)
c_v	volumetric heat capacity of the fabric (kJ/m^3K)
c_{vf}	volumetric heat capacity of the fiber (kJ/m^3 K)
c_{vg}	volumetric heat capacity of the vapor (kJ/m^3K)
c_{vl}	volumetric heat capacity of the liquid water (kJ/m^3K)
C^*	saturated water vapor concentration (kg/m^3)
C_f	water vapor concentration in the fibers of the fabric (kg/m^3)
C_g	water vapor concentration in the air filling the inter-fiber void space (kg/m^3)
C_{ab}	water vapor concentration of the ambient air (kg/m^3)
C_{fs}	water vapor concentration at the fiber surface (kg/m^3)
d_c	effective radius of the pore in fabrics (m)
D_f	diffusion coefficient of water vapor in the fibers of the fabric (m^2/s)
D_g	diffusion coefficient of water vapor in the air of the fabric (m^2/s)
D_l	diffusion coefficient of liquid water in the fabric (m^2/s)
g	acceleration of gravity (m/s^2)
h_c	convection mass transfer coefficient (m/s)
$h_{l\to g}$	mass transfer coefficient (m/s)
h_t	convection heat transfer coefficient (W/m^2 K)
K_0	Kozeny constant
K_{mix}	thermal conductivity of the fabric (W/m K)
L	thickness of the fabric (m)
$\dot{m}$	mass flux of liquid moisture through the capillaries (kg/m^2s)
m_0	total number of capillaries in porous textiles
$\dot{M}$	total mass flow rate of liquid moisture through the porous textiles (kg/s)
p	pressure in the capillary (N/m^2)
r	radial co-ordinate of a fiber (m)
r_c	capillary radius in fabrics (m)
R_c	critical capillary radius in fabrics (m)
R_f	radius of fibers (m)
S_0	shape factor (1/m)
S''_v	specific volume of the fibers (1/m)
t	real time from change in conditions (s)
T	temperature of the fabric (K)
T_{ab}	temperature of the ambient air (K)
W_c	water content of the fibers in the fabric ($W_c = C_f/\rho$)
x	x-coordinate

Greek symbols

ε	porosity of the fabric
ε_f	volume fraction of fibers
ε_g	volume fraction of water vapor
ε_l	volume fraction of liquid phase
λ	latent heat of evaporation of water(kJ/kg)
λ_l	heat of sorption or desorption of liquid water by fibers (kJ/kg)
λ_v	heat of sorption or desorption of vapor by fibers (kJ/kg)
ρ	density of the fibers (kg/m^3)
ρ_l	density of the liquid water (kg/m^3)
τ_g	effective tortuosity of the fabric for water vapor diffusion
τ_l	effective tortuosity of the fabric for liquid water diffusion
β	the average angle of the capillaries in fabrics
η	dynamic viscosity (kg/ms)
σ	surface tension (N/m)
ϕ	contact angle

where K_0 is the Kozeny constant, S_0 a shape factor, and ε the porosity. B is the permeability of the porous media, which is determined by the type of porous media and the pore geometry. Later Jackson and James [1] studied the permeability of fibrous porous media. Davis and James [2] used the analytical techniques to find the permeability of a model of a fibrous porous medium. In his research the model is an array of thin annular disks periodically spaced in planes normal to the flow, where the repeating unit is a square or an equilateral triangle, and the planes are uniformly spaced in the flow direction. The solution of Stokes equations for flow through the array is found by the method of distributed singularities, and the drag on the disk is estimated by asymptotic technique. From the drag, the flow resistance or permeability of the array is found. By matching the thin disks to thin rings, the array simulates fibrous materials like filters. In order to investigate the impacts of the arrays of fibers on the liquid flow in the porous textiles Howells [3] studied the motion of a Newtonian fluid through a sparse random array of small fixed rigid objects. Drummond and Tehir [4] researched the laminar viscous flow through regular arrays of parallel solid cylinders. Sangani [5] and his coworkers investigated the slow flow past periodic arrays of cylinders with application to heat transfer. Furthermore, they [6] studied the transport processes of the Viscous flow in random arrays in cylinders. The results show that minimum permeability generally occurs

for the most uniform pore distribution. The conclusions are agreement with our investigation. More recently, Li and Zhu [7,8] developed a mathematical model that takes into account the coupled heat and moisture transfer processes with consideration of vapor diffusion, fiber moisture sorption, condensation/evaporation and liquid transport by capillary actions. In these researches clusters of parallel fibers twisted up form pores of linear distribution in porous textiles. Later they studied a model [9] of the liquid water transfer coupled with moisture and heat transfer in porous textiles with consideration of the influence of gravity. Detailed mathematical analysis is carried out to describe the capillary actions and gravity effects of liquid water. On the basis of a fractional volume of fluid (VOF) method, the distributions of the temperature, moisture concentration, and liquid water content in the porous textiles for the different degree of hygroscopicity were numerically computed by this technique.

In this paper, we study the effects of the pore size distribution and fiber diameter on the coupled heat and liquid moisture transfer in porous textiles to reveal the mechanisms of the coupling effects. The liquid transport in porous textiles can be described as a diffusion equation, which is mainly determined by the surface tension and effective capillary pore distribution and pathways. This equation is incorporated into the energy conservation equation and the mass conservation equations of water vapor and liquid water transfer, which include vapor diffusion, evaporation and sorption of moisture by fibers. A cubic-polynomial pore distribution, which is close to the experimental measurements [11], is used to replace the linear assumption [9] of the pore size distribution in porous textiles. A series of computations with systematic variation of the pore size distribution and fiber diameter are carried out to investigate the interactions between heat transfer and moisture transfer. Meanwhile, experiments were conducted to validate the model. The predictions of temperature changes during moisture transients are compared with experimental measurements. The comparison with the experimental measurements shows the superiority of this new model in resolving the coupled heat and liquid moisture transfer in porous textiles. The results illustrate that the heat transfer process is influenced by the pore size distribution and fiber diameter of the porous textiles.

2. Governing equations

In this paper we consider a porous textile slab (e.g. a fabric). The governing equations are expressed in [9]. The mass balance of the vapor is considered in Eq. (1). The mass balance of liquid phase is considered in Eq. (3). The energy balance is established in Eq. (2)

$$\frac{\partial(C_g\varepsilon_g)}{\partial t}+\varpi_1\frac{\partial(C_f\varepsilon_f)}{\partial t}-h_{l\to g}S'_v(C^*(T)-C_g)=\frac{1}{\tau_g}\frac{\partial}{\partial x}\left[D_g\frac{\partial(C_g\varepsilon_g)}{\partial x}\right] \tag{1}$$

$$c_v\frac{\partial T}{\partial t}-\varpi_1\lambda_v\frac{\partial(C_f\varepsilon_f)}{\partial t}-\varpi_2\lambda_l\frac{\partial(C_f\varepsilon_f)}{\partial t}+\lambda h_{l\to g}S'_v(C^*(T)-C_g)=\frac{\partial}{\partial x}\left[K_{mix}\frac{\partial T}{\partial x}\right] \tag{2}$$

$$\frac{\partial(\rho_l\varepsilon_l)}{\partial t}+\varpi_2\frac{\partial(C_f\varepsilon_f)}{\partial t}+h_{l\to g}S'_v(C^*(T)-C_g)=\frac{\partial}{\partial x}\left[D_l(\varepsilon_l)\frac{\partial(\rho_l\varepsilon_l)}{\partial x}\right]+b(\varepsilon_l)\cdot\frac{\partial(\rho_l\varepsilon_l)}{\partial x} \tag{3}$$

$$\varepsilon_l+\varepsilon_g+\varepsilon_f=1 \tag{4}$$

where $D_l(\varepsilon_l)$ and $b(\varepsilon_l)$ are determined by the pore size distribution in porous textiles. Detailed analysis can be found in the next section. λ_v is a heat of sorption of water vapor by fibers, λ_l is a heat of sorption of liquid water by fibers, λ is the latent heat of evaporation, $h_{l\to g}$ is the mass transfer coefficient, K_{mix} is the thermal conductivity of the fabric, D_l is the liquid diffusivity and $c_v=\varepsilon_f c_{vf}+\varepsilon_g c_{vg}+\varepsilon_l c_{vl}$

$$\varpi_1=(1-\xi)\frac{\varepsilon_g}{\varepsilon},\quad \varpi_2=1-\frac{\varepsilon_g}{\varepsilon}+\frac{\varepsilon_g}{\varepsilon}\xi$$

ϖ_1 denotes the proportion of the sorption of water vapor by fibers. ϖ_2 denotes the proportion of the sorption of liquid water by fibers. ξ is a function of the degree of saturation of liquid moisture in porous textiles. In this paper we use that $\xi=(\varepsilon_l/\varepsilon)^m$, $(m<1)$. The ratio of $\varepsilon_l/\varepsilon$ is defined as the degree of saturation of liquid moisture in porous textiles. Here $S'_v=\varepsilon_g S_v=\varepsilon_g\frac{\varepsilon_f}{\varepsilon}\xi S''_v$, $S''_v=\frac{2}{R_f}$. S''_v is the specific volume of the fibers. $C^*(T)$ is the saturated vapor concentration and solely determined by the temperature. Consider that $\varepsilon_f=1-\varepsilon=\text{const}_1>0$. We have $\varepsilon_l+\varepsilon_g=1-\varepsilon_f=\varepsilon=\text{const}_2$, $1>\varepsilon_l\geqslant 0$, $1>\varepsilon_g\geqslant 0$.

Sorption and desorption of moisture by the fibers obey the Fickian law [10],

$$\frac{\partial C_f(x,r,t)}{\partial t}=\frac{1}{r}\frac{\partial}{\partial r}\left(rD_f(x,t)\frac{\partial C_f(x,r,t)}{\partial r}\right) \tag{5}$$

where $D_f(x,t)$ is the diffusion coefficient, which has different presentation at different stages of sorption, x is the coordinate of a fiber in the given fabric and r is the radial coordinate in a fiber. The boundary condition is determined by the relative humidity of the air surrounding a fiber at x. In a fabric, $D_f(x,t)$ is a function of $W_c(x,t)$, which is dependent on the time of sorption and the location of the fiber.

The initial and boundary conditions are same as [9]. Initially, a porous textile is equilibrated to a given atmosphere of temperature and humidity, the temperature

and moisture content are uniform throughout the slab at known values.

$$\begin{aligned} &T(x,0) = T_0 \\ &C_g(x,0) = C_0 \\ &\varepsilon_l(x,0) = 10^{-9} \\ &C_f(x,0) = f(H_{a0}, T_0) \end{aligned} \tag{6}$$

Then, the boundaries of the material are exposed to two different environments: one is an unsaturated vapor environment with temperature T_0, vapor concentration C_0, and the other is a saturated liquid environment at the temperature T_0^*.

At $x = 0$, the liquid moisture is exposed to the saturated liquid moisture. We have

$$C_g(0,t) = C^*(T), \quad T(0,t) = T_0^*, \quad \varepsilon_l(0,t) = \varepsilon_{l0}$$

At $x = L$, we have the following boundary conditions to take into account the convective nature of the boundary air layers:

$$\begin{aligned} &D_g \frac{\partial(C_g \varepsilon_g)}{\partial x}|_{x=L} = -\kappa_1 h_c (C_g - C_{ab}) \\ &K_{mix} \frac{\partial T}{\partial x}|_{x=L} = -h_t (T - T_{ab}) - \kappa_2 \lambda h_{l\to g} (C^*(T) - C_{ab}) \\ &\dot{m}\varepsilon_l = \kappa_2 h_{l\to g} (C^*(T) - C_{ab}) \end{aligned} \tag{7}$$

where h_c is the convection mass transfer coefficient (m/s); h_t is the combined heat transfer coefficient (W/m^2 K), $\kappa_1 = \varepsilon_g/\varepsilon$, $\kappa_2 = \varepsilon_l/\varepsilon$. The mass transfer at $x = L$ includes two parts: moisture vapor transfer to outer atmosphere, and the evaporation of the liquid water. κ_1 denotes the proportion of the mass transfer by vapor transport, κ_2 denotes the proportion of the evaporation of the liquid water.

3. Analysis of the mechanisms of capillary action

For the following analysis, we follow the ideas in [9] and try to establish the governing equation for liquid phase in porous textiles. The porous textiles are considered as containing a very large number of yarns woven out of fibers. A yarn is made up of a cluster of fibers twisted up. The capillaries, which are interconnected, are formed by these pores in yarns woven into the porous textiles. When the liquid moisture permeates through the porous textiles, the liquid water fills the smallest millipores first, then fills smaller ones and gradually fills large pores. Let r_c denote the capillary radius. $f_p(r_c)$ denotes the accumulated number of capillaries of radius from 0 to r_c. For a continuous distribution of capillary sizes, the cumulative frequency of occurrence of capillary radii can be related to the capillary radius, in the most general form it can be rewritten as follows:

$$f_p(r_c) = \sum_{n=1}^{\infty} c_n r_c^n \tag{8}$$

where c_n, $n = 1, 2, 3, \ldots$ are constant, which are determined by the pore distribution of the porous textiles (Fig. 1).

Consider a control cell with the thickness of Δx at the location x and time t. There must be a critical radius R_c of capillary that brings water from x to $x + \Delta x$ against gravity. All the capillaries with radii smaller than R_c are full of liquid and all the others with radii greater than R_c are empty from x to $x + \Delta x$. R_c is proportional to ε_l. R_c is the function of time t and space x. The relationship between R_c and ε_l can be found in [11]. At the location x, consider the cell with the thickness of Δx. The pressure drop in capillaries can be expressed as

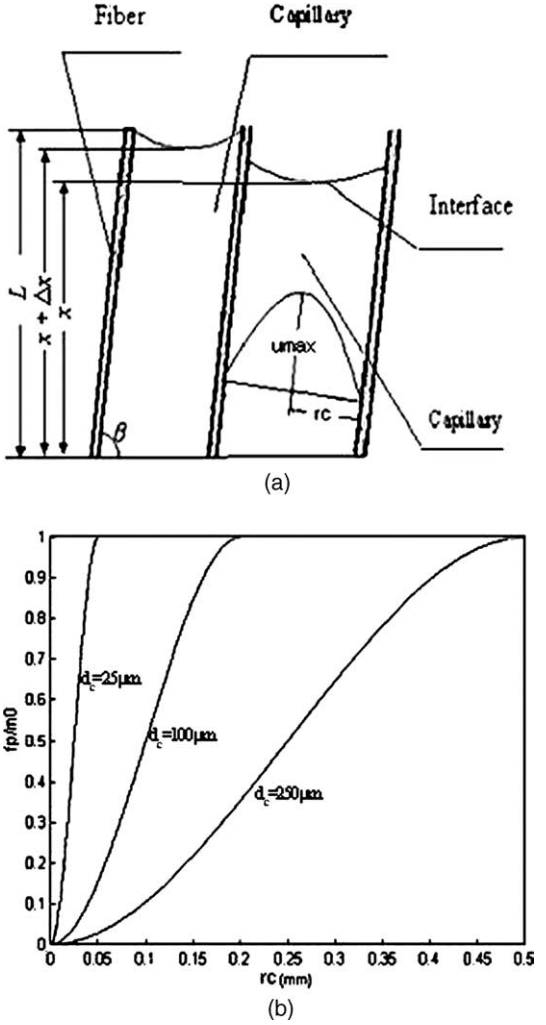

Fig. 1. (a) Schematic diagram of capillaries in porous textiles (b) $f_p(r_c)/m_0$ versus r_c.

$$\Delta p = \left(p_0 - \frac{2\sigma\cos\phi}{R_c + \Delta R_c}\right) - \left(p_0 - \frac{2\sigma\cos\phi}{R_c}\right) \tag{9}$$

Here p_0 is the air pressure, Δp is the pressure drop in capillaries. When $\Delta x \to 0$, we have

$$\frac{\partial p}{\partial x} = \frac{2\sigma\cos\phi}{R_c^2}\frac{\partial R_c}{\partial x} \tag{10}$$

By using Darcy's Law, the equation can be written as follows:

$$\dot{m} = -\psi\left(\frac{\partial p}{\partial x} + \rho_l g\right) \tag{11}$$

Here ψ is the permeability coefficient and it is generally a function of x and t, g is acceleration of gravity and ρ_l is the density of liquid water.

We have the following equation:

$$\frac{\partial(\rho_l\varepsilon_l)}{\partial t} = -\frac{\partial(\dot{m}\varepsilon_l)}{\partial x} \tag{12}$$

If Eq. (10)–(12) are compared, we can obtain the following equation:

$$\frac{\partial(\rho_l\varepsilon_l)}{\partial t} = 2\sigma\cos\phi\frac{\partial}{\partial x}\left(\frac{\varepsilon_l\psi}{R_c^2}\frac{\partial R_c}{\partial x}\right) + \rho_l g\frac{\partial(\varepsilon_l\psi)}{\partial x} \tag{13}$$

The pressure drop through a given capillary of radius r_c ($r_c < R_c$) can be written by using the Hagen–Poiseuille's Law,

$$-\frac{\partial p}{\partial x} - \rho_l g = \frac{8u_c\eta}{\sin\beta r_c^2} \tag{14}$$

For simple fabric structure, β is the effective angle of the fabric, which is the angle between the capillaries and the surface of the fabric. It is usually around 20°. u_c is the local capillary mean velocity of the water. The total mass flow rate of liquid water in the porous textile can be expressed in terms of local velocity and capillary radius r_c as follows:

$$\dot{M} = \int_0^{R_c} \rho_l u_c \sin\beta\,\mathrm{d}A_c \tag{15}$$

where A_c is cross-sectional flow area and is defined as follows: $A_c = \pi\int_0^{f_p(R_c)} r_c^2/\sin\beta\,\mathrm{d}f_p$. From above equation we have

$$\dot{M} = \int_0^{R_c} \rho_l u_c \pi r_c^2 f_p'(r_c)\,\mathrm{d}r_c \tag{16}$$

$$\dot{m} = \frac{\dot{M}}{A_c} = \sin\beta\rho_l\frac{\int_0^{R_c} u_c r_c^2 f_p'(r_c)\,\mathrm{d}r_c}{\int_0^{R_c} r_c^2 f_p'(r_c)\,\mathrm{d}r_c} \tag{17}$$

Eq. (17) can be rewritten as follows:

$$\dot{m} = -\rho_l\left(\frac{2\sigma\cos\phi}{R_c^2}\frac{\partial R_c}{\partial x} + \rho_l g\right)\frac{\sin^2\beta}{8\eta} \times \frac{\sum_{n=1}^{\infty}\frac{n}{n+4}c_n R_c^{n+4}}{\sum_{n=1}^{\infty}\frac{n}{n+2}c_n R_c^{n+2}} \tag{18}$$

For the specific fabric, c_n, $n = 1, 2, 3\ldots$ are constant, which are determined by the pore size distribution of the fabric.

According to Eq. (12), we have that

$$\begin{aligned}\frac{\partial\varepsilon_l}{\partial t} &= \frac{\partial}{\partial x}\left[\left(\frac{2\sigma\cos\phi}{R_c^2}\frac{\partial R_c}{\partial x} + \rho_l g\right) \times \frac{\varepsilon_l\sin^2\beta}{8\eta}\frac{\sum_{n=1}^{\infty}\frac{n}{n+4}c_n R_c^{n+4}}{\sum_{n=1}^{\infty}\frac{n}{n+2}c_n R_c^{n+2}}\right] \\ &= \frac{\partial}{\partial x}\left(\frac{\varepsilon_l\sigma\cos\phi\sin^2\beta}{4\eta}\frac{\sum_{n=1}^{\infty}\frac{n}{n+4}c_n R_c^{n-1}}{\sum_{n=1}^{\infty}\frac{n}{n+2}c_n R_c^{n-1}}\frac{\partial R_c}{\partial x} + \frac{\varepsilon_l\rho_l g\sin^2\beta}{8\eta}R_c^2\frac{\sum_{n=1}^{\infty}\frac{n}{n+4}c_n R_c^{n-1}}{\sum_{n=1}^{\infty}\frac{n}{n+2}c_n R_c^{n-1}}\right)\end{aligned} \tag{19}$$

Taking into account the moisture sorption/desorption into fibers and evaporation/condensation of the water, the governing equation for the liquid phase in porous textiles can be derived.

Analyze the following cases:

I. Uniform pore size distribution

In this case $R_c(\varepsilon_l) = d_c = \text{const.}$, the whole radii of pore in porous textiles are d_c, $\frac{\partial p}{\partial x} = \frac{2\sigma\cos\phi}{R_c^2}\frac{\partial R_c}{\partial x} = 0$. It leads to the diffusion coefficient of liquid water into the porous textiles is zero. It is difficult for the liquid moisture diffusion in the porous textiles. Actually in this case the surface tension of the liquid flow in porous textiles is equilibrated in all directions. The liquid flow transport in porous textiles is determined by gravity and the difference between the advancing and receding contact angles.

II. Linear pore size distribution

In this case $f_p(r_c) = c_1 r_c$, where $c_1 = \frac{m_0}{d_{c\max}}$, the relationships between the degree of saturation of liquid moisture and critical radius R_c in the fabrics are nonlinear. However, in the most cases it can be considered quasi-linear. We assume that $R_c(\varepsilon_l) = \frac{d_{c\max}}{\varepsilon}\varepsilon_l$. Eq. (19) can be rewritten as follows:

$$\frac{\partial\varepsilon_l}{\partial t} = \frac{\partial}{\partial x}\left(\frac{3\varepsilon_l\sigma\cos\phi\sin^2\beta d_{c\max}}{20\eta\varepsilon}\frac{\partial\varepsilon_l}{\partial x}\right) + \frac{9g\sin^2\beta\rho_l d_{c\max}^2\varepsilon_l^2}{40\eta\varepsilon^2}\frac{\partial\varepsilon_l}{\partial x} \tag{20}$$

Furthermore, we have

$$D_l(\varepsilon_l) = \frac{3\sigma\cos\phi\sin^2\beta d_{c\max}\varepsilon_l}{20\eta\varepsilon}$$

$$b(\varepsilon_l) = \frac{9g\sin^2\beta\rho_l d_{c\max}^2\varepsilon_l^2}{40\eta\varepsilon^2} \tag{21}$$

where ε is the porosity of the porous textile and $d_{c\max}$ is the largest effective radius of the capillaries. It is consistent with [9]. We use the radius d_c of the most capillaries in porous textiles to replace $d_{c\max}$, $d_{c\max} = 2d_c$. Eq. (21) can be rewritten as follows:

$$D_l(\varepsilon_l) = \frac{3\sigma\cos\phi\sin^2\beta d_c\varepsilon_l}{10\eta\varepsilon}$$

$$b(\varepsilon_l) = \frac{9g\sin^2\beta\rho_l d_c^2\varepsilon_l^2}{10\eta\varepsilon^2} \tag{22}$$

In [9] we proposed a dimensionless number, named GS number, $\mathrm{GS} = \frac{b(\varepsilon_l)\cdot L}{D_l(\varepsilon_l)} = \frac{3\varepsilon_l\rho_l d_c g L}{\sigma\cos\phi\varepsilon}$, to measure to ratio of gravity to surface tension. When GS number is large enough, the gravity prevails in the porous textile. It is difficult that the porous textile adsorbs liquid water. When GS is small enough, the surface tension force prevails in the porous textile. It is easy that the porous textile adsorbs liquid water.

III. Cubic-polynomial pore size distribution

In this case

$$f_p(r_c) = \frac{3m_0}{4d_c^2}r_c^2 - \frac{m_0}{4d_c^3}r_c^3,\quad 0 \leqslant r_c \leqslant 2d_c,\quad R_c(\varepsilon_l) = \frac{2d_c}{\varepsilon}\varepsilon_l$$

Eq. (19) can be expressed as

$$\frac{\partial\varepsilon_l}{\partial t} = \frac{\partial}{\partial x}\left(\frac{\sigma\cos\phi\varepsilon_l\sin^2\beta d_c}{2\eta\varepsilon}\frac{\frac{1}{5}c_1+\frac{1}{3}c_2R_c+\frac{3}{7}c_3R_c^2}{\frac{1}{3}c_1+\frac{1}{2}c_2R_c+\frac{3}{5}c_3R_c^2}\frac{\partial\varepsilon_l}{\partial x} + \rho_l g\frac{\varepsilon_l\sin^2\beta}{8\eta}R_c^2\frac{\frac{1}{5}c_1+\frac{1}{3}c_2R_c+\frac{3}{7}c_3R_c^2}{\frac{1}{3}c_1+\frac{1}{2}c_2R_c+\frac{3}{5}c_3R_c^2}\right) \tag{23}$$

Here $c_1 = 0$, $c_2 = \frac{3m_0}{4d_c^2}$, $c_3 = -\frac{m_0}{4d_c^3}$. Furthermore, Eq. (23) can be rewritten as follows:

$$\begin{aligned}\frac{\partial\varepsilon_l}{\partial t} &= \frac{\partial}{\partial x}\left(\frac{5\sigma\cos\phi\varepsilon_l\sin^2\beta d_c}{21\eta\varepsilon}\frac{7\varepsilon-6\varepsilon_l}{5\varepsilon-4\varepsilon_l}\frac{\partial\varepsilon_l}{\partial x} + \rho_l g\frac{5\sin^2\beta}{21\eta}\frac{d_c^2\varepsilon_l^3}{\varepsilon^2}\frac{7\varepsilon-6\varepsilon_l}{5\varepsilon-4\varepsilon_l}\right)\\ &= \frac{\partial}{\partial x}\left(\frac{5\sigma\cos\phi\varepsilon_l\sin^2\beta d_c}{21\eta\varepsilon}\frac{7\varepsilon-6\varepsilon_l}{5\varepsilon-4\varepsilon_l}\frac{\partial\varepsilon_l}{\partial x}\right) + \rho_l g\frac{5\sin^2\beta d_c^2\varepsilon_l^2}{21\eta\varepsilon^2}\frac{105\varepsilon^2-176\varepsilon\varepsilon_l+72\varepsilon_l^2}{(5\varepsilon-4\varepsilon_l)^2}\frac{\partial\varepsilon_l}{\partial x}\end{aligned} \tag{24}$$

We have

$$D_l(\varepsilon_l) = \frac{5\sigma\cos\phi\varepsilon_l\sin^2\beta d_c}{21\eta\varepsilon}\frac{7\varepsilon-6\varepsilon_l}{5\varepsilon-4\varepsilon_l}$$

$$b(\varepsilon_l) = \rho_l g\frac{5\sin^2\beta d_c^2\varepsilon_l^2}{21\eta\varepsilon^2}\frac{105\varepsilon^2-176\varepsilon\varepsilon_l+72\varepsilon_l^2}{(5\varepsilon-4\varepsilon_l)^2}$$

Since $0 \leqslant \varepsilon_l \leqslant \varepsilon$, $D_l(\varepsilon_l) \geqslant 0$, $b(\varepsilon_l) \geqslant 0$. Similarly, we propose another dimensionless number, named GS2 number, to measure the ratio of gravity to surface tension. It is expressed as follows,

$$\mathrm{GS2} = \frac{b(\varepsilon_l)\cdot L}{D_l(\varepsilon_l)} = \frac{\rho_l g d_c\varepsilon_l}{\varepsilon\sigma\cos\phi}\frac{105\varepsilon^2-176\varepsilon\varepsilon_l+72\varepsilon_l^2}{(5\varepsilon-4\varepsilon_l)(7\varepsilon-6\varepsilon_l)}L$$

When GS2 number is large enough, the gravity prevails in the porous textile. When GS2 is small enough, the surface tension force prevails in the porous textile.

4. Numerical solutions and discussion

4.1. Computational results

We implemented numerical simulations for several porous textile materials made of polyester. The grid orientation and numerical methodology have been reported previously [9]. The initial conditions are: $T_0 =$ 20 °C, RH = 65%. At the time $t = 0$ a sudden boundary condition changes at the surface $x = 0$ to RH = 100% and $T = 19.5$ °C. The relative humidity and temperature of the air surrounding the fabric at $x = L$ are 65% and 20 °C, respectively. The mass transfer coefficient h_c is 0.137m/s and the heat transfer coefficient h_t is 8.1 W/m^2 K at $x = L$. In the porous textile the mass transfer coefficient $h_{l\to g}$ equals to 0.137 m/s [16]. The pore size distributions can be considered as cubic-polynomial distributions.

Fig. 2 shows the predicted water vapor concentration distribution during the moisture diffusion into the void space in the polyester fabrics: (a) $d_c = 25$ μm, (b) $d_c =$ 250 μm. Fig. 2 illustrates that the diffusion of water vapor into the porous textiles through the void space in fabrics is a fast process with a transient period of increasing pulse of water vapor concentration, which is related to the fiber diameter. The transient period with the large fiber diameter is insignificant comparing with those with the small one. Also, the peak of water vapor concentration decreases with fiber diameter for both pore size distributions of the fabrics. The transient period is almost invisible for all polyester fabrics with different fiber diameter. Comparatively, The transient periods, however, are slightly significant in polyester fabrics with small fiber diameter. For both of the pore size distribution, the smaller the fiber diameter is, the more significant the transient period is.

Fig. 3 shows the distribution of the volume fraction of the liquid during the liquid water penetration into

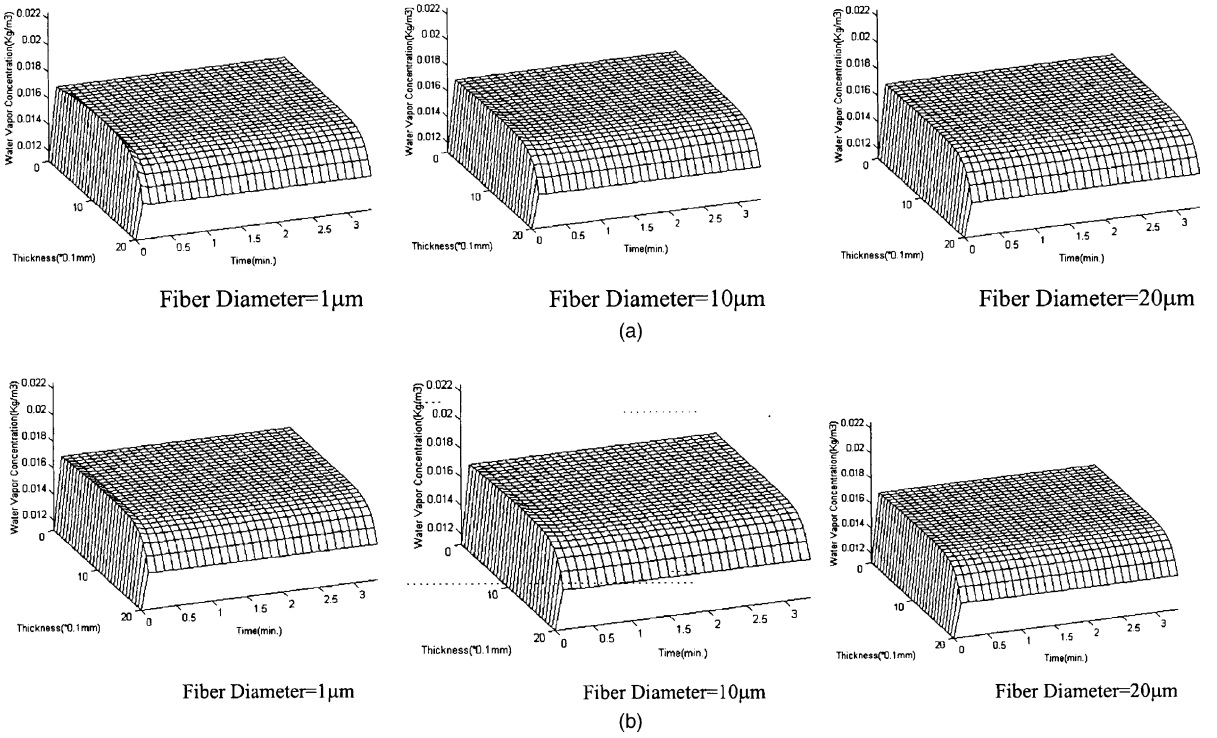

Fig. 2. (a) Distribution of water vapor concentration in the void space for the pore distribution ($d_c = 25$ μm) and (b) distribution of water vapor concentration in the void space for the pore distribution ($d_c = 250$ μm).

polyester fabrics. Comparing with the diffusion of water vapor in the void space, the penetration of the liquid water into the fabrics by capillary action is also very fast for given material properties. The liquid volume fraction reaches equilibrium very quickly in all the fabrics.

As shown in Fig. 3(a), the equilibrium of volume fraction of liquid diffused into the fabrics with the effective pore radius of $d_c = 25$ μm has the same pattern in this type of fabrics with the different fiber diameter. Meanwhile, the transient period for liquid diffusion in this fabric is the same for all the type of fabrics with different fiber diameter.

Similar patterns are observed for the fabrics with the effective pore radius of $d_c = 250$ μm, as Fig. 3(b) shows. Comparatively, the liquid water diffusion into this type of fabric due to capillary action tends to be faster than that into the first type of fabrics, as the diffusion coefficient of the liquid moisture $D_l(\varepsilon_l) = \frac{5}{21}\frac{d_c}{\varepsilon}\frac{\sin^2\beta}{\eta}\frac{7\varepsilon-6\varepsilon_l}{5\varepsilon-4\varepsilon_l}\varepsilon_l\sigma\cos\phi$ is larger in this case. For this type of fabric, it takes shorter time to reach the steady-state than the first type of fabric. The smaller the effective pore radius d_c is, the more uniform the pore distribution. The results show that minimum permeability generally occurs for the most uniform pore size distribution.

The distributions of the moisture content in the fibers are shown in Fig. 4. From the Fig. 4, we can see that the process of the water diffusion into the fibers takes longer time to reach equilibrium in fabrics with large fiber diameter. Compared with the process of the liquid water diffusion into the porous fabric due to capillary action, the process of the moisture diffusion into fibers is a relatively slow process. The liquid water is propelled into the porous textiles so rapid that the surfaces of the fibers are covered with the liquid water within 1 s for these fabrics. The process of the water diffusion into fibers across the thickness of the porous textiles almost starts at the same time, but takes about 3.5 min to reach equilibrium for the fabric with fiber diameter of 20 μm, and about 0.1 min for the fabric with fiber diameter of 1 μm. Fig. 4 shows that the distributions of moisture content in the fibers across the thickness of the porous textiles are almost uniform due to the almost uniform distribution of liquid water in the fabrics. The pore size distribution in fabrics does not have significant influence on the sorption of moisture by the fibers.

Fig. 5 shows the temperature distributions in the fabrics during the liquid moisture diffusion process. Fig. 5(a) illustrates that the temperature rises initially in the inner layers of the fabrics, then decreases gradually and reaches equilibrium with the environment. The maximum temperature rise during the transient period decreases with fiber diameter. For the small fiber diameter

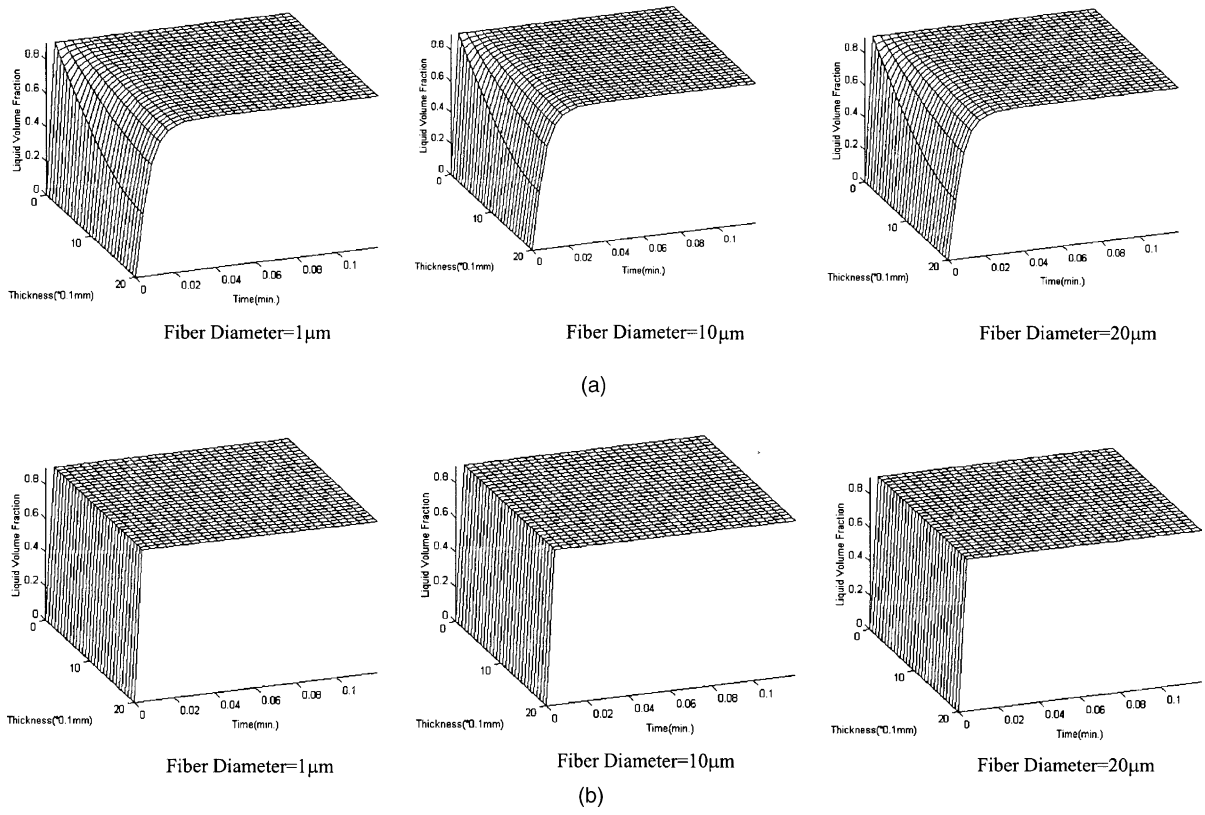

Fig. 3. (a) Distribution of the liquid volume fraction for the pore distribution ($d_c = 25$ μm) and (b) distribution of the liquid volume fraction for the pore distribution ($d_c = 250$ μm).

the temperature rise with the same fiber diameter is substantially the highest at the case of the effective pore radius $d_c = 25$ μm. For the large fiber diameter the temperature rise shows similar pattern for all the fabrics. It indicates that the fiber diameter and pore size distribution of the fabrics are the factors determining the coupling effect between heat and moisture transfer processes.

The initial rise in temperature is due to the heat released during moisture sorption by the fibers. The heat absorbed during the evaporation of liquid water also affects the temperature. When the time is less than 0.5 min for the fabrics with small fiber diameter, the heat rate of sorption is significant, so that the temperature rises rapidly. For the first type of fabrics the differences in temperature between fibers in the middle and at surfaces of the fabric vary from 0.1 to 5.5 °C, depending on the fiber diameter of the fabrics. For the second type of fabrics, the temperature differences vary from 0.1 to 2.5 °C. The smaller the fiber diameter of the fabric is, the more the heat rate of sorption is released, so that the higher the temperature rise is. When $t \geqslant 1$ min, the temperature distribution becomes steady and uniform across the thickness of the fabrics.

4.2. Comparison with experiments

To investigate the effects of the pore size distribution and fiber diameter on the coupled heat and liquid moisture transfer in porous textiles, a series of experiments were carried out by using the porous materials with different pore size distributions and fiber diameters. The fabric sample, which is initially equilibrated to the ambient of conditions of 20 °C and 65%RH, is put on a container filled with water at 19.5 °C. Some filter papers are put in the container to prevent the fabric from sinking. An infrared camera is used to measure the temperature changes at the upper surface of the fabrics during the transient processes. The improved model was applied to these fabrics used in the experiment. The characteristics of the fabrics are shown in Table 1.

As Fig. 6a shows, the computational and experimental results for the porous textiles with fiber diameter 10 μm and $d_c = 25$ μm. Fig. 6b shows the computational and experimental results for the porous textiles with fiber diameter 20 μm and $d_c = 25$ μm. Fig. 6c shows the computational and experimental results for the porous textiles with fiber diameter 10 μm and $d_c = 250$ μm. Fig. 6d shows the computational and experimental results for

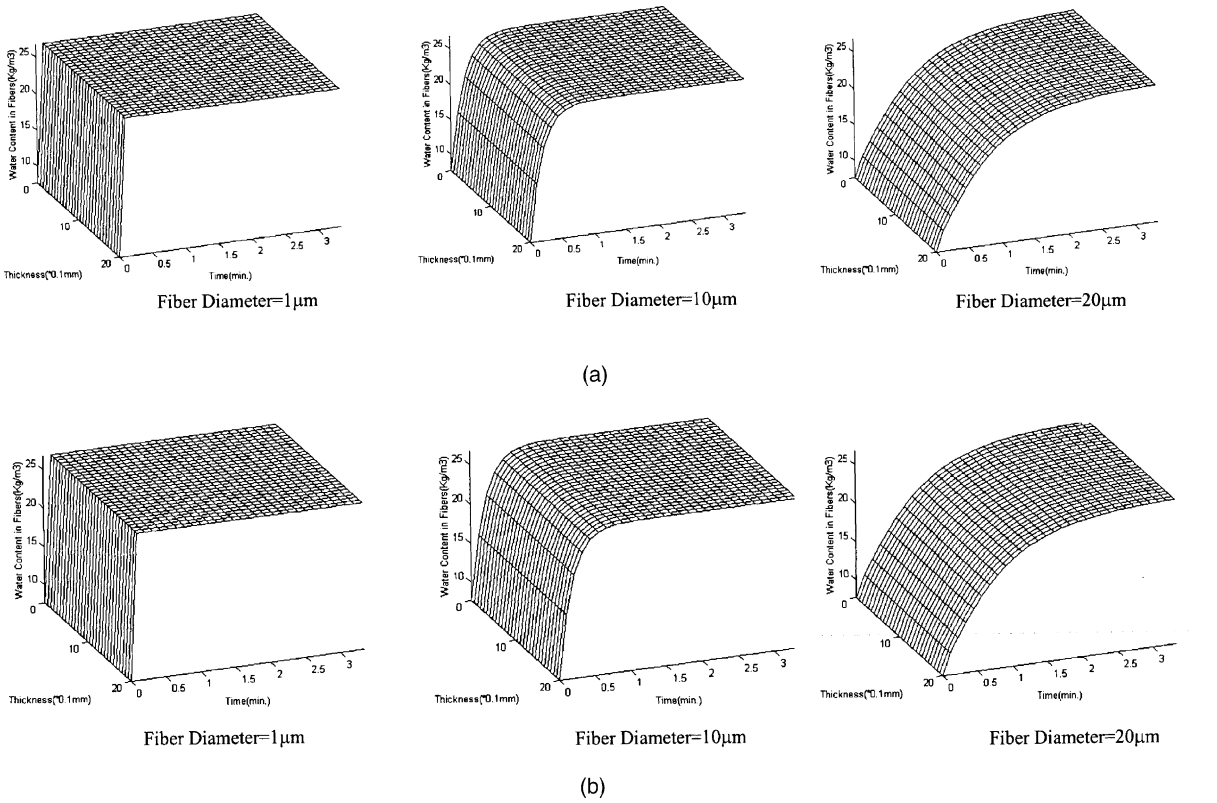

Fig. 4. (a) Distribution of the water content in the fibers of the polyester fabrics for the pore distribution ($d_c = 25$ μm) and (b) distribution of the water content in the fibers of the polyester fabrics for the pore distribution ($d_c = 250$ μm).

the porous textiles with fiber diameter 20 μm and $d_c = 250$ μm. Line a is numerical results derived by the improved mathematical model. Line b is numerical results obtained by the mathematical model in [9]. There are good agreements between the numerical solutions and the experimental measurements. The comparison with the experimental measurements shows the superiority of this new model in resolving the coupled heat and liquid moisture transfer in porous textiles.

4.3. Discussions

The theoretical computational results and the experimental measurements illustrate the impact of heat transfer process on the moisture transfer processes, including moisture transfer by water vapor diffusion, liquid capillary action, and the moisture sorption of the fibers. As Fig. 3 shows, the water diffusion through the air filling the inter-fiber void space is a fast process, which is effected by the liquid diffusion process and the heat transfer processes, as shown in Figs 3 and 5. Comparing Fig. 2 with Fig. 5, the water vapor concentrations in the fabrics have the same patterns of variations as the temperature distributions across different fiber diameter and the pore size distribution, because the saturated water vapor concentration is a function of temperature. For all polyester fabrics the transient period is almost invisible.

The liquid diffusion is determined by a number of factors: the surface tension σ, contact angle ϕ, average angle β, viscosity η, volume fraction of liquid water ε_l, the pore size distribution as defined by formula $D_l(\varepsilon_l) = \frac{5}{21}\frac{d_c}{\varepsilon}\frac{\sin^2\beta}{\eta}\frac{7\varepsilon-6\varepsilon_l}{5\varepsilon-4\varepsilon_l}\varepsilon_l\sigma\cos\phi$. When the contact angle is smaller than 90°, liquid water can diffuse into the fabric and can be a fast process as shown in Fig. 3. When the contact angle is greater than 90°, D_l is smaller than and/or equal to 0, indicating that the liquid water cannot diffuse into the fabric. The heat transfer process does not affect the liquid diffusion process significantly, as the liquid volume distributions in Fig. 3 are quite independent of the temperature distributions in Fig. 5.

The evaporation process is also influenced by the liquid transport process. When the liquid water cannot diffuse into the fabric, the liquid water can only evaporate at the lower surface of the fabric. As the liquid diffuses into the fabric due to capillary action, the

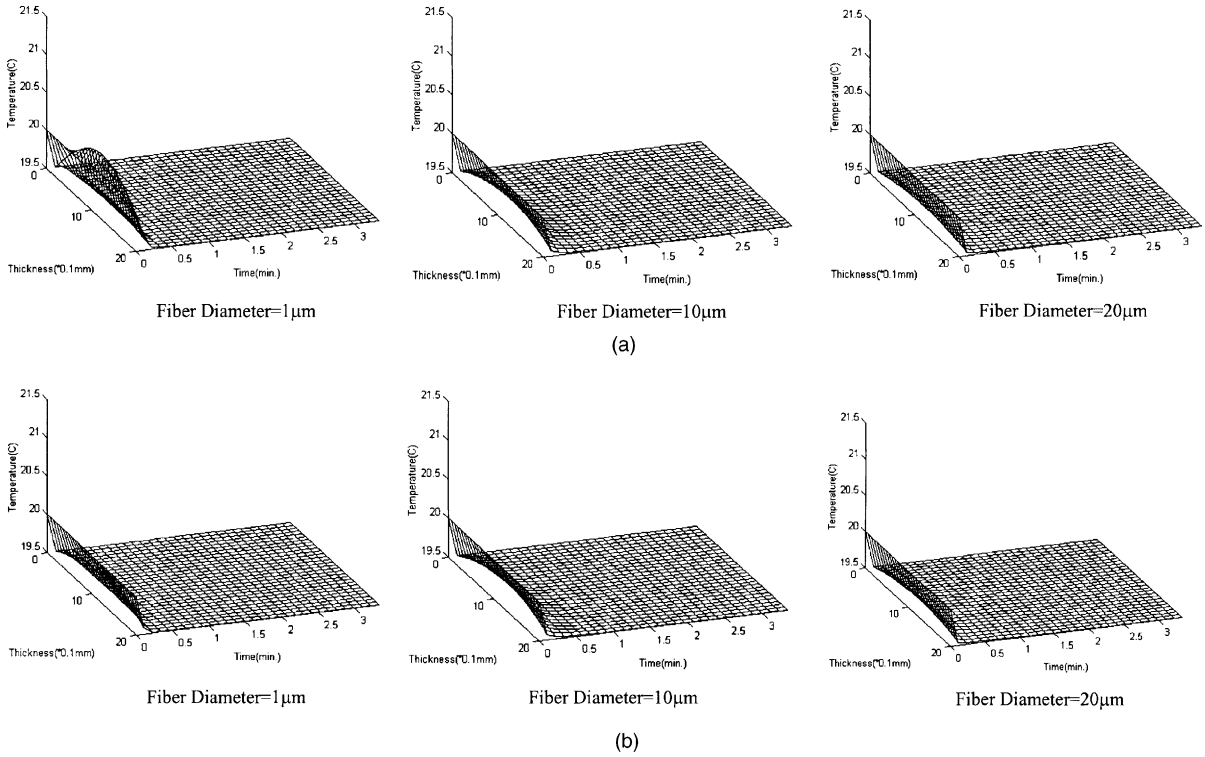

Fig. 5. (a) Temperature distribution in the polyester fabrics for the pore distribution ($d_c = 25$ μm) and (b) temperature distribution in the polyester fabrics for the pore distribution ($d_c = 250$ μm).

Table 1
Fabrics used in the experiments and numerical simulation

Fiber	Fabric thickness (mm)	Fiber diameter (μm)	Pore size distribution (d_c) (μm)
Polyester	2	1	25
Polyester[a]	2	10	25
Polyester[a]	2	20	25
Polyester	2	1	250
Polyester[a]	2	10	250
Polyester[a]	2	20	250

[a] Denotes the experimental observation and numerical simulation.

evaporation can take place throughout the fabric. The heat transfer process is affected by the fiber diameter. In the fabrics with the fiber diameter of 1 μm, the large temperature differences between the middle layers and surface layers are shown in Fig. 5a.

The process of moisture sorption is largely affected by the water vapor diffusion, the liquid water diffusion processes but not by the heat transfer process. When there is liquid diffusion in the fabric, the moisture sorption of fibers is mainly determined by the liquid transport process as shown in Fig. 4, as the fiber surfaces are covered by liquid water very quickly. All the moisture transport processes, on the other hand, also affect the heat transfer process. The temperature rise during the transient period is caused by the balance of heat released during fiber moisture sorption and the heat absorbed during the evaporation process.

In the first type of fabrics the diffusion coefficient of the liquid moisture is the smallest. It means that the proportion of liquid water in the first type of fabrics is the least during the transient period. It is well known that the heat capacity of liquid water is large. On the other hand, the heat released during liquid moisture sorption by the fibers in the fabrics with the small fiber diameter is more than these fabrics with the large fiber diameter. In Fig. 5 we can see that the temperature rise with the fiber diameter of 1 μm in the first type of fabrics is the highest.

As a whole, a dry piece of fabric exhibits three stages of transport behavior in responding to external humid transients. The first stage is dominated by two fast processes: water vapor diffusion and liquid water diffusion in the air filling the inter-fiber void space, which can reach new steady-states within a fraction of seconds. During this period, the water vapor diffuses into the

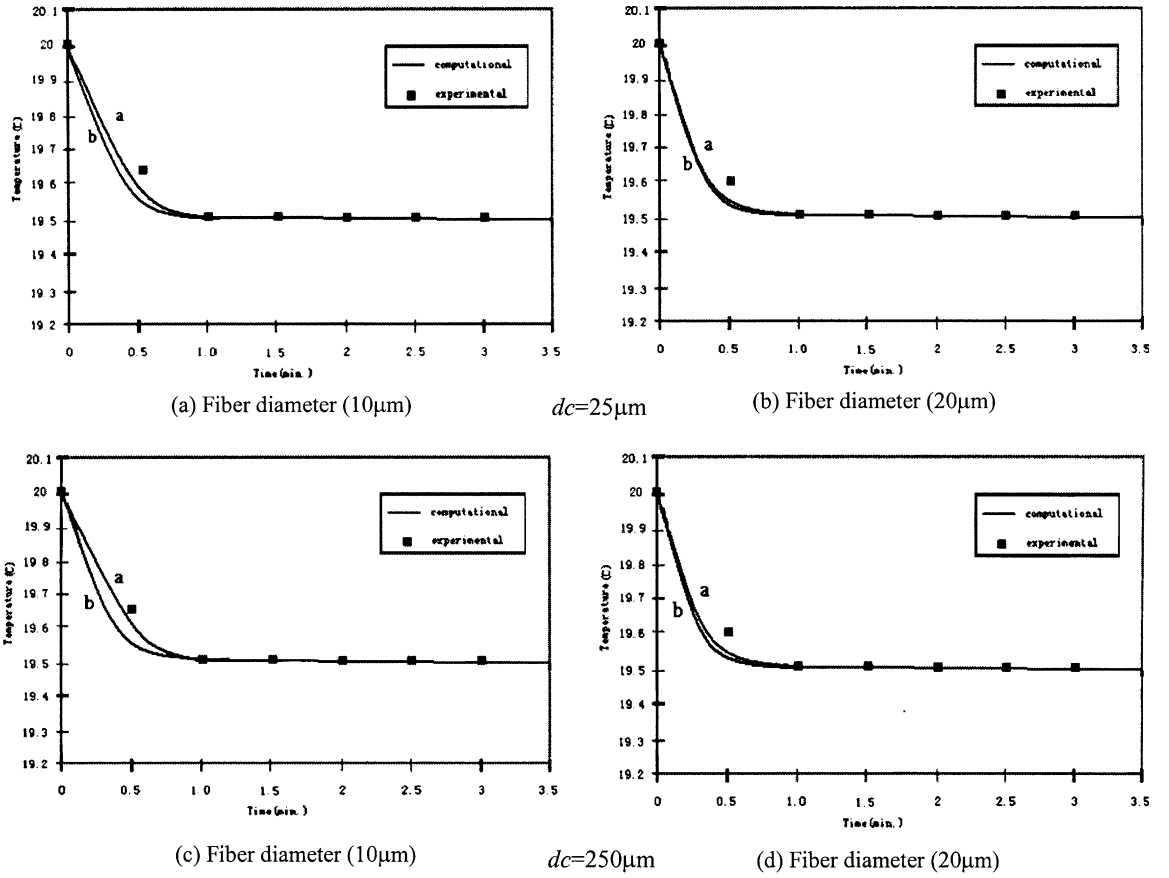

Fig. 6. Comparison of computed temperature changes at fabric upper surface with experimental measurements.

fabric due to the concentration gradient across the two surfaces. Meanwhile, the liquid water starts to flow out of the regions of higher liquid content to the drier regions by the surface tension force. For the porous fabrics the capillary distribution is very complicated. The liquid transport can be a rapid process, which takes about $\tau \sim L^2/D_l$ to fill the porous media, where L is the thickness of the media. In other words, all the fibers in the porous textile will be covered with the liquid water rapidly when one surface of the fabric contacts the liquid water.

The second stage is featured by the moisture sorption of fibers, which is a relatively slow process and takes a few minutes to a few hours to complete. In this period, the sorption of the water into the fibers takes place as the water vapor diffuses into the fabric, which increases the relative humidity at the surfaces of fibers. After liquid water diffuses into the fabric, the surfaces of the fibers are saturated due to the film of water on the surfaces of the fibers, which again will enhance the sorption process. During these two transient stages, the heat transfer process is coupled with the four different forms of liquid transfer processes due to the heat released or absorbed during the sorption/desorption and evaporation/condensation. The sorption/desorption and evaporation/condensation processes, in turn, are affected by the efficiency of heat transfer.

Finally, the third stage is reached as a steady-state, in which all the four forms of moisture transport and the heat transfer process become steady and the coupling effects among them become less significant. The distributions of temperature, water vapor concentration, fiber water content and volumetric fraction of liquid water become invariant in time. With the evaporation of the liquid water at the upper surface of the fabrics, the liquid water is drawn from capillaries to the upper surface.

5. Conclusion

This paper focuses on a theoretical investigation of the coupling mechanism of heat transfer and liquid moisture diffusion in porous textiles by using an improved mathematical model. In this model, the pore size

Table 2
Physical properties of the materials

Parameters	Symbol	Unit	Polyester
Density of fibers [12]	ρ	kg/m^3	1.38×10^3
Radius of fibers	R_f	m	1.0×10^{-5}
Porosity of fabric	ε		0.88
Diffusion coefficient of vapor in a fiber	D_f	m^2/s	3.9×10^{-13}
Volumetric heat capacity of fabric [13]	C_{vf}	kJ/m^3 K	$4.184\times10^3\times1.38\times(0.32+W_c/1.0+W_c)$
Thermal conductivity of fabric [14]	K_{mix}	$\times10^{-3}$ W/m K	$40.4+23.0W_c$
Heat of sorption of vapor [15]	λ_v	kJ/kg	2522.0
Heat of sorption of liquid [15]	λ_l	kJ/kg	2260.0
Surface tension	σ	N/m	29×10^{-3}–33×10^{-3}
Contact angle	ϕ		75°

distribution is assumed to be a cubic-polynomial distribution, which is close to the experimental measurements [11]. The liquid diffusion behavior in porous textiles can be described as a diffusion equation. The improved diffusion coefficient can be expressed as: $D_l(\varepsilon_l)=\frac{5}{21}\frac{d_c}{\varepsilon}\frac{\sin^2\beta}{\eta}\frac{7\varepsilon-6\varepsilon_l}{5\varepsilon-4\varepsilon_l}\varepsilon_l\sigma\cos\phi$. This equation is incorporated into the energy conservation equation and the mass conservation equations of water vapor and liquid water transfer, which include vapor diffusion, evaporation and sorption of moisture by fibers. With specification of initial and boundary conditions, a series of computed results were derived for polyester fabrics with different diameter of the fibers and pore size distribution. The predictions of temperature changes during moisture transients are compared with experimental measurements, good agreement is observed between the two. The comparison with the experimental measurements shows the superiority of this new model in resolving the coupled heat and liquid moisture transfer in porous textiles. Analysis of the computational and experimental results illustrates that the heat transfer process is influenced by the pore size distribution and fiber diameter of the porous textiles.

Acknowledgements

We would like to thank the National Natural Science Foundation of China Grant 10102024 and the Hong Kong Polytechnic University for the funding of this research.

Appendix. Numerical relationships and values of fiber–fabric properties

In the computations, the values of the material properties are listed in Table 2. The values with references are obtained from literature, and those without reference are measured values.

References

[1] G.W. Jackson, D.F. James, The permeability of fibrous porous media, Can. J. Chem. Eng. 64 (1986) 364–374.
[2] A.M.J. Davis, F. James, Slow flow through a model fibrous porous medium, Int. J. Multiphase Flow 22 (5) (1996) 969–989.
[3] I.D. Howell, Drag due to the motion of a newtonian fluid through a sparse random array of small fixed rigid objects, J. Fluid Mech. 64 (1974) 449–475.
[4] J.E. Drummond, M.I. Tehir, Laminar viscous flow through regular arrays of parallel solid cylinders, Int. J. Multiphase Flow 10 (1984) 515–540.
[5] A.S. Sangani, A. Acrivos, Slow flow past periodic arrays of cylinders with application to heat transfer, Int. J. Multiphase Flow 8 (1982) 193–206.
[6] A.S. Sangani, C. Yao, Transport processes in random arrays in cylinders II, viscous flow, Phys. Fluids 31 (1988) 2435–2444.
[7] Y. Li, Q. Zhu, Simultaneous heat and moisture transfer with moisture sorption, condensation and capillary liquid diffusion in porous textiles, Text. Res. J. 73 (6) (2003) 515–524.
[8] Y. Li, Q. Zhu, K.W. Yeung, Influence of thickness and porosity on coupled heat and liquid moisture transfer in porous textiles, Text. Res. J. 72 (5) (2002) 435–446.
[9] Y. Li, Q. Zhu, A model of coupled liquid moisture and heat transfer in porous textiles with consideration of gravity, Numer. Heat Transfer, Part A 43 (5) (2003) 501–523.
[10] Y. Li, Z. Luo, An improved mathematical simulation of the coupled diffusion of moisture and heat in wool fabric, Text. Res. J. 69 (10) (1999) 760–768.
[11] B. Miller, I. Tyomkin, An extended range liquid extrusion method for determining pore size distributions, Text. Res. J. 56 (1) (1986) 35–40.
[12] M. Yao, Textile Material, 1st ed., Textile Industry Press, Beijing, China, 1980.
[13] A. Rae, B. Rollo, The WIRA Textile Data Book, WIRA, Leeds, UK, 1973.
[14] A.M. Schneider, Heat transfer through moist fabrics, Ph.D. Thesis, University of New South Wales, Kensington, NSW, Australia, 1987.

[15] B.H. Billings, D.E. Gray (Eds.), American Institute of Physics Handbook, 2nd ed., McGraw-Hill, London, UK, 1972, pp. 4–190.

[16] Y. Li, A.M. Plante, B.V. Holcombe, Fiber hygroscopicity and perceptions of dampness part II: physical mechanisms, Text. Res. J. 65 (6) (1995) 316–324.